



Removal of VOC from water by pervaporation with hollow-fiber silicone rubber membrane module

Jingli Xu, Akira Ito*

*Department of Chemical Engineering, Tokyo Institute of Technology, Ookayama 2-12, Tokyo 152-8552, Japan.
Tel. +81357342151; Fax +8135734215; email: aito@chemeng.titech.ac.jp*

Received 20 July 2009; accepted 22 November 2009

ABSTRACT

A pervaporation process was used to remove dissolved volatile organic compounds (VOC) (benzene and toluene) from water using a hollow-fiber membrane module of silicone rubber with a 60- μm membrane thickness and 0.37- m^2 membrane area. The effect of water feed rate and feed temperature on removal efficiency was investigated. For a feed concentration of 200 ppm, the removal efficiency of benzene could reach 90% up to a water feed rate of 70 cm^3/min , but the removal efficiency of toluene was only 72% at a water feed rate of 50 cm^3/min . When the feed temperature was increased, the removal was more effective. A degassing experiment was performed to test the effect of dissolved air on the removal efficiency. The existence of dissolved air enhanced the removal efficiency of VOC from water. The permeabilities of VOC vapor with or without water vapor were measured by a vapor permeation experiment. With water vapor, the permeabilities of the VOC decreased. A calculation model based on the Henry constant and permeability was proposed and predicted the experimental results well.

Keywords: Silicone rubber; Hollow-fiber membrane; VOC; Pervaporation

1. Introduction

Most of the industrial countries encounter problems caused by groundwater and surface water pollution by volatile organic compounds (VOC). Conventional methods for separation of VOC include air-stripping [1], adsorption using activated carbon [2], biological treatment [3], catalytic oxidation [4] and distillation. These processes have drawbacks such as high-energy consumption, costly regeneration steps, etc. In the last 10 years, much research on the separation of VOC from water has focused on membrane technology such as nanofiltration [5,6], reverse osmosis [7], pervaporation (PV) [8–12], membrane distillation [13–15], membrane

air-stripping process [16,17] and the combination of a membrane process with biological treatment [18,19].

Among these technologies, PV is a promising process for the separation of VOC from water because of the compact design, recycling of recovered VOC and no emission problem. The PV is a separation process in which a liquid mixture is separated by means of selective vaporization through a non-porous membrane [11]. The driving force of the permeation is the difference in the vapor pressure between the feed liquid and the permeated vapor.

The membranes used in the PV process are mostly hydrophobic materials, which favor VOC preferential permeation. The most used membrane is a silicone rubber composite membrane, where silicone rubber is formed onto a microporous support. The silicone rubber has very good stability in operation and the

*Corresponding author

selectivity for VOC relative to water is high [11]. In addition to the silicone rubber composite membrane, there are several other membranes used in VOC removal from aqueous solution. For example, Jian et al. [20] have studied the separation of dilute organic–water mixtures using a flat sheet membrane module with a poly(vinylidene fluoride) membrane. Ho et al. [21] have reported the removal of organics from aqueous solution using a supported polyglycol liquid membrane. Liu et al. [22] have done research on separation of organics/water with a zeolite membrane.

Among the research studies on VOC removal by PV, a plate-and-frame module is commonly used, but it is expensive and leakage through the gasket is a serious problem. A hollow-fiber module not only can compensate for this disadvantage but also has unique characteristics. An advantage of the hollow-fiber module is the ability to pack a very large membrane area into a single module.

In this study, a hollow-fiber silicone rubber membrane module with a 60- μm thickness was used to remove dissolved VOC in water at a low concentration of 200 ppm by PV. The removal performance from water of VOC, such as benzene and toluene, was measured. The effect of feed flow rate, feed temperature and dissolved air in the solution on removal efficiency was demonstrated. The calculation models were proposed to explain the experimental results based on the vapor permeability.

2. Experimental

2.1. PV

Fig. 1a shows the PV experimental setup for removing of VOC, benzene or toluene, from water. The experimental apparatus consisted of a pure water vessel (15 L), a VOC-saturated solution vessel (1 L), a membrane module, a diaphragm vacuum pump (N820.3, KNF Neuberger GmbH, Germany) and a treated water vessel.

The membrane module was a hollow-fiber membrane module (M60-3000, Nagayanagi Co., Ltd, Japan) with an effective length of 15.1 cm using 3,000 dense silicone rubber hollow fibers of 60- μm thickness and 340- μm diameter. The membrane area of the module was 0.37 m^2 .

The concentration of the VOC in the feed water was about 200 ppm that was adjusted by controlling the mixing fraction of the VOC-saturated solution. Pure water was aerated with air constantly, and the feed rate was changed from 20 to 150 cm^3/min . The VOC solution was prepared prior to the start of the experiment

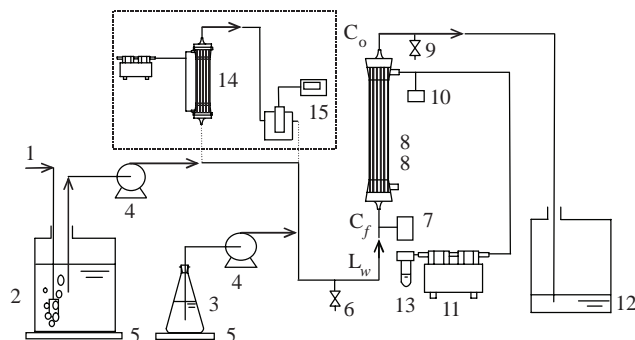


Fig. 1. (a) 1: Air, 2: Pure water vessel, 3: VOC saturated water vessel, 4: Feed pump, 5: Heating plate, 6: Inlet sampling port, 7: Thermometer, 8: Hollow-fiber silicone rubber membrane module, 9: Outlet sampling port, 10: Pressure gauge, 11: Diaphragm vacuum pump, 12: Treated water vessel, 13: Vapor trap, 14: Membrane contactor, 15: DO meter.

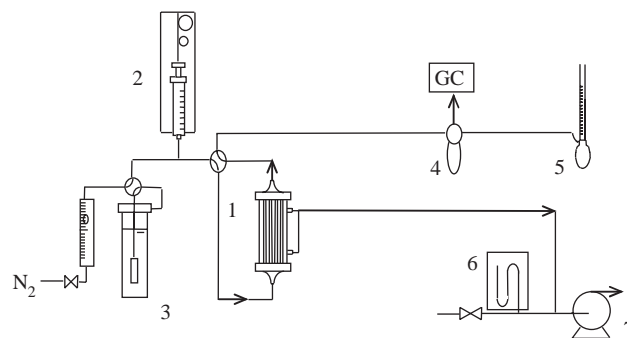


Fig. 1. (b) 1: Hollow-fiber membrane module, 2: Micro-feeder, 3: Water vapor saturator, 4: Gas sampling, 5: Soap film flowmeter, 6: Manometer, 7: Vacuum pump.

Experimental setup: (a) PV and (b) Vapor permeation.

by mixing pure water with a small amount of benzene or toluene for 24 h and the concentration on the vessel nearly reached at its saturation concentration, which is shown in Table 1.

To test the effect of dissolved air on the removal efficiency, another experiment with a degassed feed was done. For degassing the feed water, a membrane contactor with a porous hydrophobic hollow-fiber membrane (Liqui-Cel G478, Celgard Inc., U.S.A.) and a pump system were inserted into the water feed line (the rectangular part in Fig. 1a). By evacuation with the pump, the feed water was degassed after passing through the membrane contactor. To determine the degassing level, a DO meter was used. For pure water feed, after degassing, the concentration of oxygen was lowered from 8 to 9 ppm, which was the saturation concentration, to below 0.2 ppm. After the degassed water was mixed with the VOC-saturated solution, the dissolved air concentration in the feed was around 10%

Table 1
Parameters and properties

	Benzene	Toluene	O ₂	N ₂	Water
<i>H</i> [kPa/ppm]	0.0061 (293K)	0.0021 (293 K) 0.0060 (298 K) 0.012 (302 K) 0.020 (305 K)			
<i>H'</i> [kPa/mol frac.] [27]			4.0×10^6 (293 K)	8.1×10^6 (293 K)	
<i>D</i> _{AB} [m ² /s] (293 K)	1.02×10^{-9}	9.15×10^{-10}			
Solubility [ppm] (293 K)	1,830	530			
<i>Q</i> [kmol m/(s m ² kPa)]	3.0×10^{-12}	2.9×10^{-12}	1.2×10^{-13} [25]	6.7×10^{-14} [25]	5.5×10^{-12} [25]

of the saturation concentration, namely, 0.8 ppm-O₂ and 1.5 ppm-N₂.

The feed water containing VOC was fed to the lumen side of the silicone rubber membrane module. The shell side of the membrane module was kept at 1.75 kPa, which was nearly the saturated water vapor pressure at the operation temperature of 293 K. For a dissolved toluene feed, the experiment was done under different temperature of 293–306 K.

The whole experimental run time was 1–3 h. For each run, after a run of 30 min or more, water samples at the inlet and outlet were taken from the sample ports and analyzed by a FID gas chromatograph (GC-14B, Shimadzu Corporation, Japan). The accuracy of the GC analysis was under 5 ppm absolute VOC concentration. The concentration at the inlet, *C_f*, and the outlet, *C_o*, was the average value of the sampling results for several times. The VOC removal efficiency in this report means decreasing the level from *C_f* to *C_o*.

2.2. Vapor permeation

To measure the vapor permeability of VOC through the silicone rubber hollow-fiber membrane, a vapor permeation (VP) experiment was performed. The experimental setup is shown in Fig. 1b. It consisted of a mini hollow-fiber module (Nagayanagi Co., Ltd. Japan), a water vapor saturator, a micro-feeder and a vacuum pump.

The membrane material of the mini module was the same as that of the module used in the PV experiment. The mini hollow-fiber module with an effective length of 5.2 cm was made up of 3,000 fine silicone rubber hollow fibers providing an area of 0.081 m². The membrane thickness was 20 μm. The outer diameter of each fiber was 190 μm, and the inner diameter was 150 μm.

The feed vapor consisted of nitrogen and 0.06–0.8% toluene or benzene vapor. Toluene or benzene was fed

by a micro-feeder and evaporated to be mixed with nitrogen. The flow rate of nitrogen was 1 L/min. The concentration of toluene or benzene was controlled by the feed speed of the micro-feeder. Feed gas was introduced to the lumen side of the hollow-fiber membrane. The shell side was connected to a vacuum pump to keep the pressure in the permeate side at 0.4 kPa. The experiment was done at 293 K.

To test the effect of the co-permeating water vapor on the VOC permeability, experiments with a feed containing saturated water vapor were also carried out. The feed nitrogen passing through the water vapor saturator was mixed with VOC and was fed to the membrane module. The concentrations of VOC at the inlet and outlet in the feed side of the membrane module were measured by a gas chromatograph (GC-14B Shimadzu Corporation, Kyoto, Japan) with TCD.

2.3. Henry constant

The Henry constant of benzene or toluene dissolved in water was measured by an aeration experiment according to our previous study [15]. A 1 L -VOC aqueous solution, the initial concentration of which was 500 ppm-VOC, was aerated with dry air at 293 K. The water sample was collected every five minutes and was analyzed by a gas chromatograph until the concentration became low. From the reducing curve of the concentration, the Henry constant was estimated.

3. Results and discussion

3.1. VOC removal by PV

Fig. 2 shows the experimental results of removal of the dissolved benzene from water by PV at 293 K. Benzene concentration at the inlet, *C_f*, and the outlet, *C_o*, of the membrane module were plotted vs the water feed flow rate. For example, at an air-saturated water feed of 100 cm³/min, the benzene concentration at the inlet,

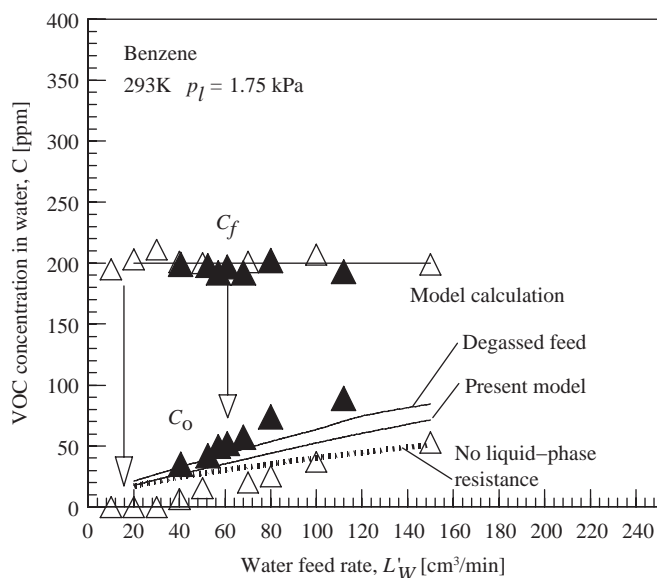


Fig. 2. Removal of dissolved benzene from water using silicone rubber hollow-fiber membrane module. \triangle : feed with dissolved air, \blacktriangle : degassed feed.

207 ppm, was reduced to 37 ppm at the outlet of the membrane module. When the water feed rate was under $30 \text{ cm}^3/\text{min}$, the dissolved benzene at the outlet was not detected. The removal efficiency could reach above 90% up to a water feed rate of $70 \text{ cm}^3/\text{min}$. With the increasing water feed rate, the concentration of benzene in water at the outlet also increased. The increasing water feed rate lowered the removal efficiency.

When using a degassed or no-air contained feed, the concentration of benzene at the outlet was found to increase. For example, at a water feed rate of $40 \text{ cm}^3/\text{min}$, the concentration of benzene at the outlet increased from 5 to 35 ppm. The dissolved air in the feed water had an effect on the removal efficiency of VOC from water. The presence of dissolved gas in the feed water enhanced the removal efficiency.

The experimental results for the removal of toluene from water by PV at 293 K are shown in Fig. 3. When the water feed rate was $50 \text{ cm}^3/\text{min}$, the removal efficiency was only about 72%. The removal efficiency of the module for benzene and toluene was different. Under the same PV experimental conditions, the removal efficiency of the module for toluene was low compared to that for benzene. This is attributed to the low Henry constant, H , of toluene as shown in Table 1.

The effect of feed temperature on the removal efficiency is shown in Fig. 4 for a toluene aqueous solution feed. With the increasing temperature, the concentration of toluene at the outlet of the membrane module decreased. When the feed temperature reached 306 K, the toluene in water could be removed thoroughly.

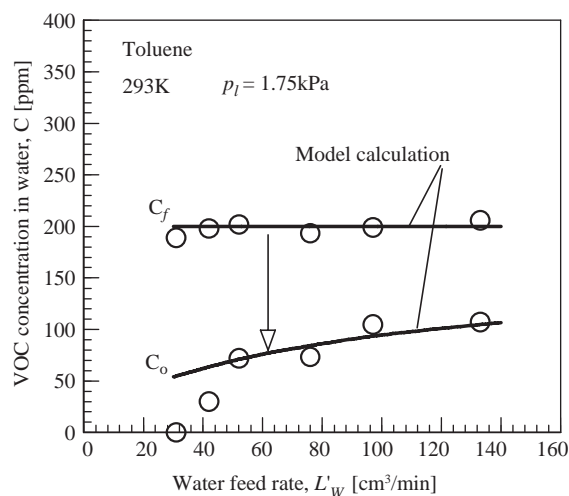


Fig. 3. Separation of dissolved toluene from water using silicone rubber hollow-fiber membrane module.

This meant that the increasing feed temperature increased the removal efficiency of toluene, namely a higher feed temperature was beneficial for the removal of toluene. This is because increasing the feed temperature caused the equilibrium vapor partial pressure to increase, consequently resulting in the driving force increase.

3.2. Model calculation

A three-step mechanism will describe the mass transfer process in the present PV process: (1) the

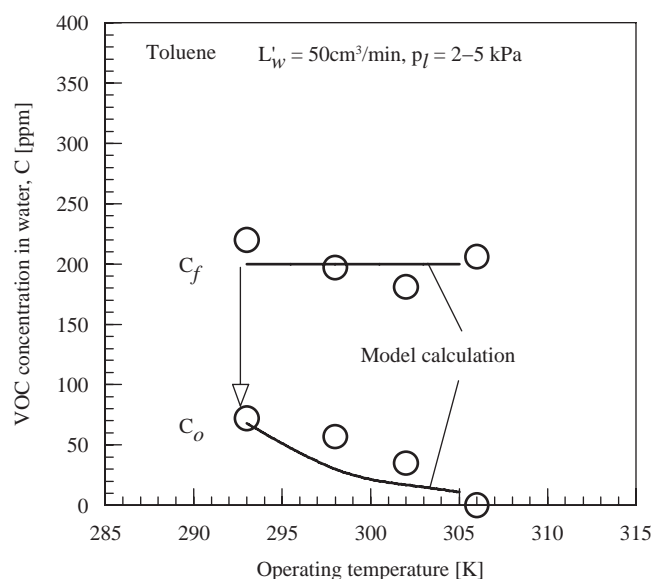


Fig. 4. Effect of operating temperature on the separation performance for dissolved toluene in water.

diffusion of permeate component from bulk water to the membrane surface (liquid phase resistance), (2) the evaporation of components at the water–membrane interface, where the VOC vapor, water vapor and air exist at their partial vapor pressure, and (3) the VP through the membrane material (VP). The permeate-side mass transfer resistance could be negligible because of the low-vacuum condition. The process parameters of the steps are discussed as follows.

3.2.1 Liquid phase resistance

The flow condition of the feed water was laminar in the hollow fiber. For a laminar flow with parabolic velocity profile in a tube, the liquid-phase mass transfer resistance of the feed side could be estimated by the Hausen equation [23]:

$$Sh_d^* \equiv \frac{(dL_{VOC}/dA)d}{cD_{AB}(x_i - x)} = 3.66 + \frac{0.0668[(d/l)Re_dSc]}{1 + 0.04[(d/l)Re_dSc]^{2/3}} \quad (1)$$

The diffusivity of VOC in water, D_{AB} , was estimated according to the Wilke-Chang correlation [24] and is listed in Table 1. For example, when the feed flow rate, L_w , is 50 cm³/min and the bulk concentration of VOC, C , is 107 ppm, the Reynolds number, Re_d , is 1.8 and the Sherwood number, Sh_d^* , is 3.8. The calculated VOC concentration in water at the membrane surface, x_i , is 2.15×10^{-5} , while the bulk concentration, x , is 2.45×10^{-5} . This means that the liquid-phase resistance was around 10% of the total mass transfer resistance in the present PV process.

3.2.2. Partial vapor pressure of VOC

The partial vapor pressure of dissolved VOC plays an important role in the mass transfer process. According to Henry's law, the partial vapor pressure of VOC at the feed water surface is related to the concentration of the VOC in water:

$$p^*_{VOC} = HC_{VOC,i} = H'x_i, \quad (2)$$

where H is the Henry constant. The Henry constants measured in this study are shown in Table 1. For toluene, the Henry constants at different temperatures are also shown. The water temperature has a large effect on the Henry constant of the VOC.

3.2.3. Vapor permeability

The vapor permeability of benzene or toluene through the silicone rubber hollow-fiber membrane

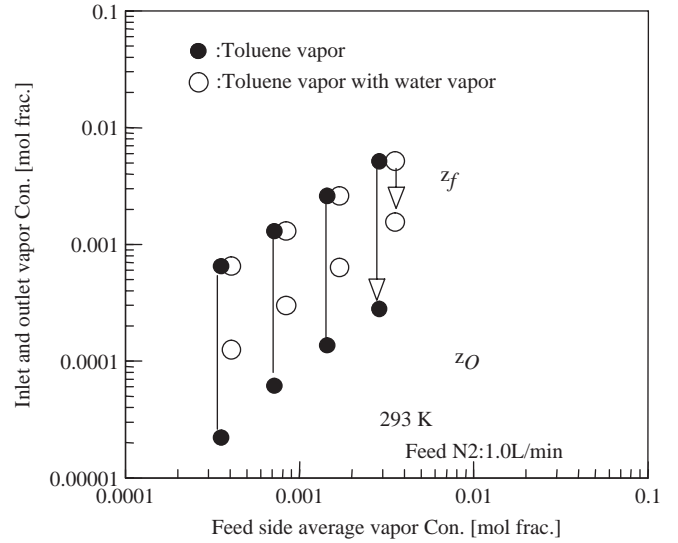


Fig. 5. Vapor permeation results for toluene vapor in nitrogen.

was measured in a VP experiment, and the results for toluene vapor with and without water vapor are shown in Fig. 5. The vapor concentrations in the feed gas at the inlet and the outlet were plotted vs the feed side average vapor concentration. When the vapor concentration in the feed gas, z_f , was 0.0014, the concentration at the outlet, z_o , was 0.000141. For the feed gas with water vapor, when z_f was 0.0016, z_o was 0.000654. The co-permeation of water vapor decreased the VOC permeability.

The permeability for the VOC vapor, Q , was evaluated by fitting a model calculation to the vapor permeation result. The fitting model was based on plug-flow in the feed side and complete mixing in the permeate side as follows:

$$(dF_{VOC}/dA) = -(Q_{VOC}/\delta)(p_h z - p_l y_p), \quad (3)$$

$$(dF_{N_2}/dA) = -(Q_{N_2}/\delta)(p_h(1 - z) - p_l(1 - y_p)), \quad (4)$$

$$z = F_{VOC}/(F_{VOC} + F_{N_2}), \quad (5)$$

where F was the feed flow rate of each component, and z was the VOC mole fraction in the feed gas. The permeability of nitrogen was 6.7×10^{-14} kmol m/(s m² kPa) [25]. For the complete-mixing model in the permeate side, the VOC mole fraction in the permeate side, y_p , was constant. This model will be applicable for a small pressure ratio, where p_l/p_h was 0.005 in the case of this measurement. The model equations were integrated 0 to the permeation area, A , to result in an outlet VOC concentration, z_o . The permeability of VOC was estimated by trial-and-error procedure.

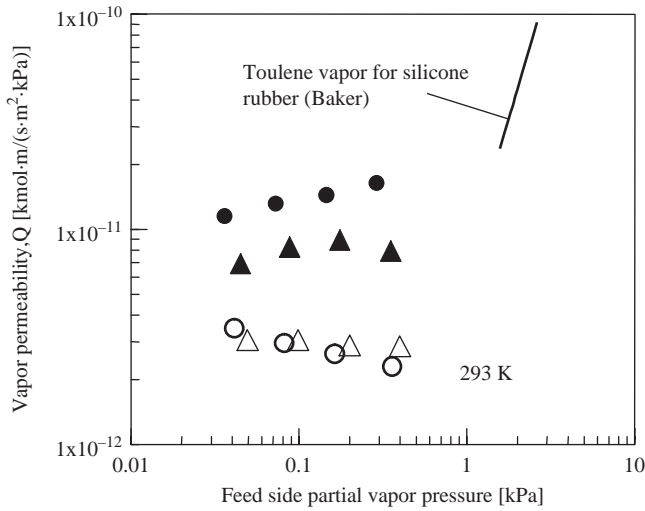


Fig. 6. Vapor permeabilities. ●: Benzene vapor, ▲: Toluene vapor, ○: Benzene vapor with water vapor, △: Toluene vapor with water vapor.

The relationship between vapor permeability and its partial pressure is shown in Fig. 6. As shown by a solid line in the figure, the permeability of vapor usually depends on the partial pressure [26], but at less than 1 kPa partial pressure, the vapor permeability dependency of partial pressure was very small. The existence of water vapor resulted in a drastic decrease in the vapor permeability of toluene and benzene. The concentration of water vapor in feed gas (2–3%) was larger than that of the VOC vapor under the experimental condition (0.1%). The water vapor in the membrane material may reduce the solubility of organic vapor to the membrane material. The existence of water vapor in the permeation process may lower the permeability of VOC vapor through silicone rubber. The permeability value with water vapor will be used in the model calculation.

3.2.4. Model calculation

For the present PV process for removing VOC from water, the model calculation was based on a co-current-flow model where both the feed stream and the permeate stream were in plug-flow. The molar flow rate of each component in the liquid feed side, L_i , and that in the permeate vapor side, V_i , are described in the differential equations as follows:

$$(dL_{\text{VOC}}/dA) = -(Q_{\text{VOC}}/\delta)(p_{\text{VOC}}^* - p_{\text{IVOC}}), \quad (6)$$

$$(dL_w/dA) = -(Q_w/\delta)(p_w^* - p_{\text{I}w}), \quad (7)$$

$$(dL_{\text{O}_2}/dA) = -(Q_{\text{O}_2}/\delta)(p_{\text{O}_2}^* - p_{\text{IO}_2}), \quad (8)$$

$$(dL_{\text{N}_2}/dA) = -(Q_{\text{N}_2}/\delta)(p_{\text{N}_2}^* - p_{\text{IN}_2}), \quad (9)$$

$$(dV_{\text{VOC}}/dA) = -(dL_{\text{VOC}}/dA), \quad (10)$$

$$(dV_w/dA) = -(dL_w/dA), \quad (11)$$

$$(dV_{\text{O}_2}/dA) = -(dL_{\text{O}_2}/dA), \quad (12)$$

$$(dV_{\text{N}_2}/dA) = -(dL_{\text{N}_2}/dA), \quad (13)$$

$$y_i = V_i / \sum V_i (i = \text{VOC}, w, \text{O}_2, \text{N}_2), \quad (14)$$

$$x_i = L_i / \sum L_i (i = \text{VOC}, w, \text{O}_2, \text{N}_2). \quad (15)$$

The permeation rate, dL_i/dA , depends on the vapor permeability and the partial pressure difference between the feed–membrane interface and the permeate side. The permeabilities of water vapor, nitrogen and oxygen through a silicone rubber membrane have been measured in our previous study [25], which are listed in Table 1. The VOC permeabilities were the mean value of the measured permeabilities as shown in Fig. 6, which are also listed in Table 1. The vapor pressure of VOC, p_{VOC}^* , was calculated from Eq. (2) with the measured Henry constant. The $p_{\text{O}_2}^*$ and $p_{\text{N}_2}^*$ were also calculated by the Henry constants shown in Table 1. The model equations were integrated from 0 to the permeation area, A , and the results of the model calculations are shown in Figs. 2–4.

In Fig. 2, the three model calculation results are shown for the feed containing 200 ppm dissolved benzene. Considering the liquid-phase mass transfer resistance, Eq. (1), the present model is shown by the solid line. If liquid-phase mass transfer resistance is neglected, $x = x_i$, the concentration of VOC at the outlet could then be calculated from Eq. (6) to Eq. (15); the result is shown by a dotted line (no liquid-phase resistance). The liquid-phase resistance was around 10% of the total mass transfer resistance, which had a minor effect on the VOC removal efficiency in the PV process.

The model for the degassed feed also predicted the effect of dissolved gas on the removal efficiency of benzene from water. For the degassed feed model, the concentration of oxygen and nitrogen in the feed water was treated as 0. The result is shown by a thin line in the figure. The present model considering co-permeation of dissolved air predicted a higher removal efficiency of benzene compared to the degassed feed model. This is due to the lowering of the partial vapor pressure of the VOC component at the permeate side caused by the permeation of dissolved air. The dissolved air in the feed will have an effect on the removal

performance of the PV process for dissolved VOC at low concentration. In the experiment, this effect was larger than that predicted, probably because the concentration of dissolved air was larger than its saturation concentration.

The result of the model calculation for toluene at 200 ppm in the feed water is shown in Fig. 3. It also predicted well the tendency of the removal of toluene from water. For a low feed rate, the concentration at the outlet was much lower than the model calculation value. The most likely reason was that toluene was probably adsorbed on the silicone rubber material of the membrane module and that the 1–3 h run time was not long enough. If the run time lasted longer, toluene would appear at the outlet.

In Fig. 4, the model calculation result for the effect of process temperature on the outlet toluene concentration is shown. As shown in Table 1, the Henry constant and vapor pressure for toluene increases with temperature. For this reason, the removal efficiency of the PV process will increase with the operation temperature. The present model calculation predicted well the effect of temperature.

4. Conclusions

The removal efficiency of dilute aqueous solutions of VOC, benzene or toluene, through a fine silicone rubber membrane and the effect factors of removal efficiency were investigated. Feed water rate, feed temperature and dissolved air in water had an effect on the removal of VOC. Higher feed water rate negated the removal of VOC from water. In contrast, higher feed temperature was beneficial for the removal of VOC. Dissolved air's presence of in the water enhanced the removal efficiency of VOC. Under the same experimental conditions, the removal efficiency of the module for benzene was better than that for toluene. The results of vapor permeation experiments showed that the presence of water vapor caused a drastic decrease in the vapor permeability through the silicone rubber membrane because water vapor in the membrane material reduced the solubility of organic vapor in the membrane material.

The model calculation based on the Henry constant and permeability predicted well the experimental results. The model explained the effect of the dissolved air and the temperature on the VOC removal efficiency.

Symbols

A	membrane area [m ²]
C	VOC concentration in water [ppm]

c	molar density of feed liquid [kmol/m ³]
D_{AB}	diffusion coefficient for dissolved VOC in water [m ² /s]
d	tube (hollow-fiber) inner diameter [m]
F	feed flow rate of nitrogen or VOC vapor [kmol/s]
H	Henry constant [kPa/ppm]
L	component flow rate in liquid feed [kmol/s]
L'_w	feed flow rate of water [cm ³ /min]
l	tube (hollow-fiber) length [m]
p_h	feed side pressure [kPa]
p_l	permeate side pressure [kPa]
p^*	vapor pressure of a component in aqueous solution [kPa]
Q	permeability of gas or vapor through silicone rubber membrane [kmol·m/(s·m ² ·kPa)]
Re_d	Reynolds number for flow in a tube [–]
Sc	Schmidt number for dissolved VOC in water [–]
Sh_d^*	Sherwood number [–]
V	component flow rate in permeate side [kmol/s]
x	VOC mole fraction in feed flow [–]
x_i	VOC mole fraction in water at membrane surface [–]
y	component mole fraction in permeate side [–]
z	VOC mole fraction in gas or vapor flow of feed side [–]
δ	membrane thickness [m]
f	feed
N ₂	nitrogen
O ₂	oxygen
o	potentate or outlet of feed side
p	permeate side
VOC	benzene or toluene
w	water

References

- [1] V. Linek, J. Sinkele and V. Janda, *Water Res.*, 32 (1998) 1264–1270.
- [2] J. Yu and S. Chou, *Chemosphere*, 41 (2000) 371–378.
- [3] J. Suschka, B. Mrowiec, *Water Sci. Tech.*, 33 (1996) 273–276.
- [4] S. K. Gangwal, M. E. Mullins, J. J. Spivey, P. R. Caffrey and B. A. Tichenor, *Appl. Catal.*, 36 (1988) 231–247.
- [5] G. Ducom and C. Cabassud, *Desalination*, 124 (1999) 115–123.
- [6] B. V. Bruggen and C. Vandecasteele, *Environ. Pollut.*, 122 (2003) 435–445.
- [7] R. Rautenbach and I. Janisch, *Chem. Eng. Process.*, 23 (1988) 67–75.
- [8] I. Blume, J.G. Wijmans and R. W. Baker, *J. Membr. Sci.*, 49 (1990) 253–286.
- [9] T. Yamaguchi, S. Yamahara, S. Nakao and S. Kimura, *J. Membr. Sci.*, 95 (1994) 39–49.
- [10] L. Hitchens, L.M. Vane and F.R. Alvarez, *Sep. Purif. Tech.*, 24 (2001) 67–84.
- [11] M. Peng, L.M. Vane and S.X. Liu, *J. Hazard. Mater.*, B98 (2003) 69–90.

- [12] T. Ohshima, Y. Kogami, T. Miyata and T. Uragami, *J. Membr. Sci.*, 260 (2005) 156–163.
- [13] F.A. Banat and J. Simandl, *Chem. Eng. Sci.*, 51 (1996) 1257–1265.
- [14] A.M. Urriaga, E.D. Gorri, G. Ruiz and I. Ortiz, *Sep. Purif. Tech.*, 22 (2001) 327–337.
- [15] S. Duan, A. Ito and A. Ohkawa, *J. Chem. Eng. Japan*, 34 (2001) 1069–1073.
- [16] A.K. Zander, M.J. Semmens and R.M. Narbaitz, *J. Am. Water Works Assoc.*, 81 (1989) 76–81.
- [17] H. Mahmud, A. Kumar, R.M. Narbaitz and T. Matsuura, *J. Membr. Sci.*, 179 (2000) 29–41.
- [18] L.M. Freitas dos Santos and A.G. Livingston, *Water Res.*, 29 (1995) 179–194.
- [19] T.A.C. Oliceira, J.T. Scarpello and A.G. Livingston, *J. Membr. Sci.*, 195 (2002) 75–88.
- [20] K. Jian, P.N. Pintauro and R. Ponangi, *J. Membr. Sci.*, 117 (1996) 117–133.
- [21] S.V. Ho, P.W. Sheridan and E. Krupetsky, *J. Membr. Sci.*, 112 (1996) 13–27.
- [22] Q. Liu, R.D. Noble, J.L. Falconer and H.H. Funke, *J. Membr. Sci.*, 117 (1996) 163–174.
- [23] A.L. Hines and R.N. Maddox, *Mass Transfer: Fundamentals and Applications*, Prentice-Hall, 1985, p. 176.
- [24] B.E. Poling, J.M. Prausnitz, J.P.O'Connell, *The Properties of Gases and Liquids*, Fifth edition, McGraw-Hill, 2001, p. 11, p. 22.
- [25] A. Ito, K. Yamagiwa, M. Tamura, M. Furusawa, *J. Membr. Sci.*, 145 (1998) 111–117.
- [26] R. W. Baker, N. Yoshioka, J. Mohr and A. J. Khan, *J. Membr. Sci.*, 31 (1987) 259–271.
- [27] R.S. Shankland, *Handbook of Chemistry and Physics*, 44th edition, CRC Press, 1962, p. 1078.